Full-field Displacement and Strain Rosettes by Moiré Interferometry

High-sensitivity fringe patterns of displacement components U_x, U_y, U_{45} are transformed to patterns of normal strain components ϵ_x, ϵ_y, ϵ_{45} by mechanical shearing

by E.M. Weissman and D. Post

ABSTRACT—A cross-line phase-type specimen grating was interrogated by moiré interferometry techniques to produce full-field fringe patterns of three displacement components: U_x, U_y and U_{45}. For U_{45}, sensitivity was 1/1700 mm/fringe (1/43,000 in./fr). Closely packed fringes with much information content were obtained. Fringe patterns of strain components ϵ_x, ϵ_y and ϵ_{45} were produced by mechanical shearing (or optical differentiation) of the displacement patterns; a shearing distance of only 0.6 mm (0.025 in.) was used. The rosette method yields complete strain information from these three components of normal strain—which were derived from three direct derivatives of displacement. Consequently, the need for cross-derivatives of displacement, which are highly sensitive to accidental rigid-body rotations, is circumvented.

List of Symbols

f, f_1, f_2 = frequency of grating
g_1, g_2, g_3 = pitch of grating
N_x, N_y, N_{45} = fringe order of contour of displacement component
N'_x, N'_y, N'_{45} = fringe order of contour of normal strain
U_x, U_y, U_{45} = displacement component
x, y = orthogonal coordinates
$x, y, 45$ = subscripts denoting direction of parent quantity
X_{45} = coordinate lying 45 deg from x-axis
α = angle of incidence (Fig. 2)
γ_{xy} = shear strain
$\delta_x, \delta_y, \delta_{45}$ = translation distance for mechanical shearing
Δ = change of
$\epsilon_x, \epsilon_y, \epsilon_{45}$ = normal strain component
λ = wavelength of coherent light

Introduction

Dantu[1] and Chiang[2] have shown that cross-line gratings of the amplitude (or bar-and-space) type also function as gratings in the ±45-deg directions. This applies for crossed-phase gratings too. Let the array of dots in Fig. 1 represent the peaks in a crossed-phase grating. Such a grating diffracts light in the same way as a linear grating that has crests and troughs of pitch g_1 lying parallel to the x-axis; simultaneously it diffracts light in the same way as a linear grating parallel to the y-axis. These diffractions depend on the orderly arrangement of repeating rows of features. However, repeating rows of features also exist in the diagonal ±45 deg directions and these act as linear diffraction gratings with pitch $g_2 = g_1/\sqrt{2}$. In fact, a great number of different repeating rows exist, and they all function as linear gratings in their respective directions. The rows shown in Fig. 1 with pitch g_3 are an example.

When used in conjunction with moiré interferometry, such gratings can yield fringes defining three normal displacement fields, e.g., U_x, U_{45} and U_y. These may be used to generate full-field patterns of normal strain components ϵ_x, ϵ_{45} and ϵ_y, by the approximate method known alternatively as optical differentiation or mechanical shearing.[1,3,4] The three strain components define the complete state of surface strain throughout the field of view; with them, shear strains γ_{xy} can be calculated by the rosette equation

$$\gamma_{xy} = 2\epsilon_{45} - (\epsilon_x + \epsilon_y) \quad (1)$$

and principal strains and maximum shear strain in the xy surface can be calculated by standard relationships.

The objectives of this work are: (1) to demonstrate that high quality patterns of U_{45} can be obtained by interrogating a crossed-phase grating along the 45-deg direction, (2) to show that moiré interferometry can produce high quality displacement patterns with extremely high information content, i.e., with very closely packed fringes, and

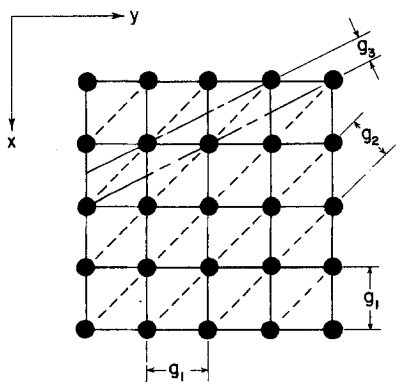

Fig. 1—Peaks on a crossed phase grating formed in regularly spaced rows of pitch g_1, g_2, g_3, etc.

E.M. Weissman and D. Post (SESA Fellow) are Graduate Student and Professor, respectively, Department of Engineering Science and Mechanics, Virginia Polytechnic Institute and State University, Blacksburg, VA 24061.

Paper was presented at 1981 SESA Spring Meeting held in Dearborn, MI on May 31-June 4.

Original manuscript submitted: June 17, 1981. Date authors notified of acceptance: August 7, 1981. Final version received: September 1, 1981.

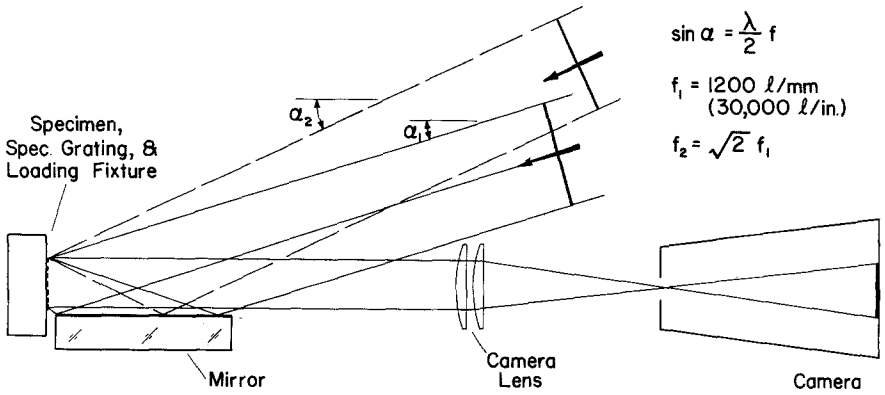

Fig. 2—Optical arrangement for these tests

(3) to demonstrate that mechanical shearing can be used with small translations to generate full-field patterns of strain components ϵ_x, ϵ_{45}, ϵ_y.

Preliminary Tests

A crossed-phase grating of 600 ℓ/mm (15,000 ℓ/in.) was formed in silicone rubber on a specimen by the method outlined in Refs. 4 and 5. The specimen was a tensile plate, 63 × 200 × 3 mm (2.5 × 8 × 1/8 in.) with a 13-mm (0.5-in.) diameter central hole. It was machined from black polymethylmethacrylate (pmma). It was mounted in a small loading fixture in juxtaposition to the optical apparatus illustrated in Fig. 2.

The apparatus is the same as that described in Ref. 6, except that a second illumination beam was provided at angle α_2. The beam incident at α_1 generated a virtual reference grating of 1200 ℓ/mm (30,000 ℓ/in.); it was used to interrogate the specimen grating in the x and y directions. The beam at α_2 generated a virtual reference grating of 1700 ℓ/mm (43,000 ℓ/in.) and was used to interrogate the diagonal specimen grating (Fig. 1) of pitch g_2 (or frequency $1/g_2$ = 850 ℓ/mm). Fringe multiplication by a factor of 2 was used.

The results are shown in Fig. 3. The method of Ref. 6 was used for each pattern, whereby a carrier of about 10 ℓ/mm (250 ℓ/in.) was introduced by rotational mismatch of the specimen and virtual reference gratings; the no-load patterns were photographed with the specimen (and loading fixture) oriented successively in the x, y and X_{45} directions; corresponding load patterns were photographed with precisely the same directions; each pair of photographic negatives was superimposed to generate the moiré pattern of load minus no-load contours; and the superimposed negatives were optically filtered to eliminate the carrier patterns and enhance contrast.

The results were fulfilling inasmuch as the quality of the U_{45} pattern was fully as good as the U_x and U_y patterns. This high quality was obtained even though it was formed with an incidental specimen grating—one that existed only as a consequence of the basic crossed grating—and even though its sensitivity was $\sqrt{2}$ or 1.41 times that of the U_x and U_y fields.

Subsequent Tests

A similar specimen, now 51-mm (2-in.) wide with a 10-mm (0.4-in.) diameter hole, was prepared with a silicone-rubber crossed grating of 600 ℓ/mm (15,000 ℓ/in.). The no-load pattern of moiré interference is shown in Fig. 4. These initial fringes were caused by imperfect uniformity of the specimen grating and the virtual reference grating.

The full-load pattern of Fig. 5 shows a substantially greater load than before, with so many displacement fringes that they are not well resolved in this figure. They are very well resolved in the camera and on the photographic negative, however, as seen in the enlarged view shown in Fig. 6. The density of fringes along the side of the hole was more than 12 fringes/mm (300 fringes/in.).

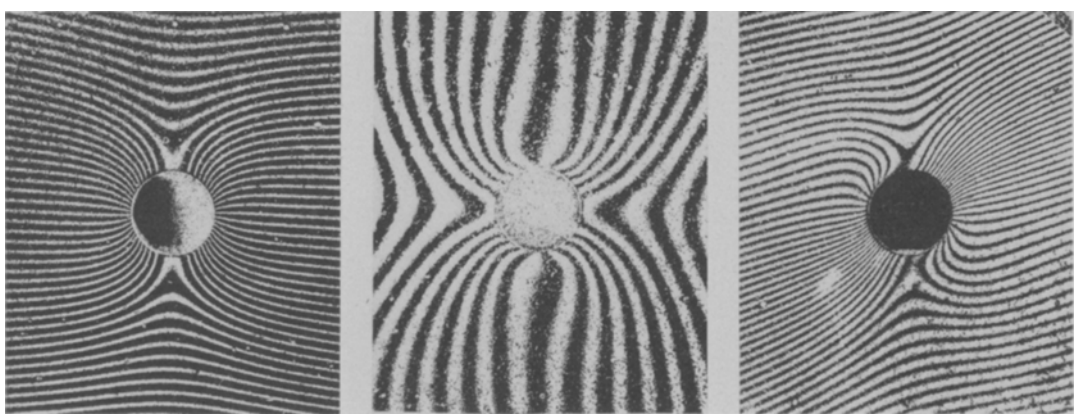

Fig. 3—Displacement fringes N_x, N_y, N_{45} (left to right) for a tensile plate with a central hole, loaded in the x direction

Fig. 4—Initial pattern (N_x) for no-load condition

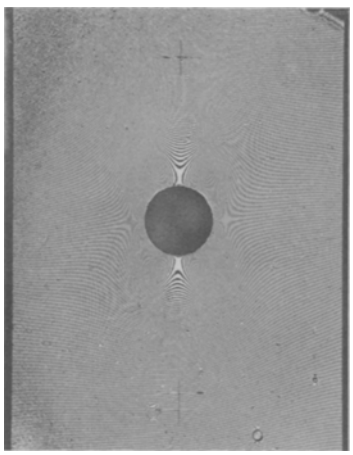

Fig. 5—Full-load pattern of displacement fringes (N_x)

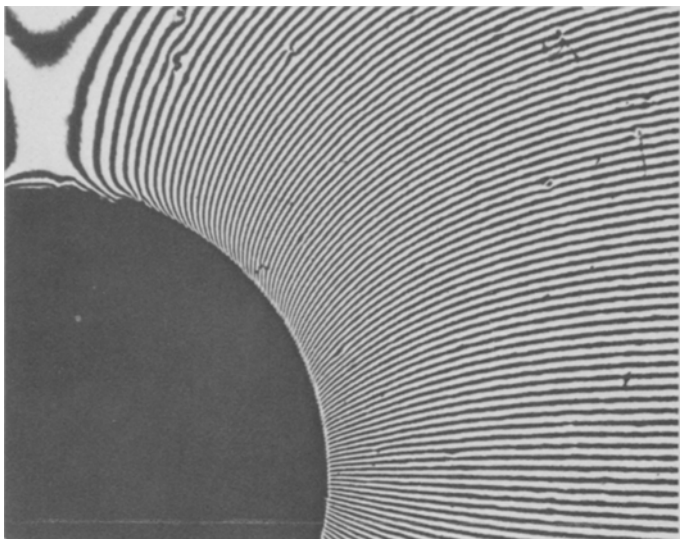

Fig. 6—Enlarged view of fringes in Fig. 5

Strain Components by Mechanical Shearing

The fringe pattern of Figs. 5 and 6 was modified by a rigid-body rotation of the specimen (and loading fixture) to add a carrier pattern of about 24 fringes/mm (600 fringes/in.). While the fringes were very closely spaced, they could still be easily resolved by the film, Kodak Contrast Process Panchromatic film.

An exposure was made. Then the film holder was translated parallel to the direction of carrier fringes—i.e., essentially perpendicular to the direction of lines of the (virtual) reference grating—and a second exposure was made on the same film. The fringes of the two superimposed (but displaced) images crossed in various zones to create a moiré pattern depicting fringes of constant $\Delta U_x/\delta_x$. This was optically filtered as described in Ref. 6 to produce the pattern of Fig. 7(a). Similarly, Figs. 7(b) and (c) show the results of mechanically shearing the displacement fields U_y and U_{45}, respectively.

Since

$$U_x = (1/f_1)N_x \tag{2}$$

and

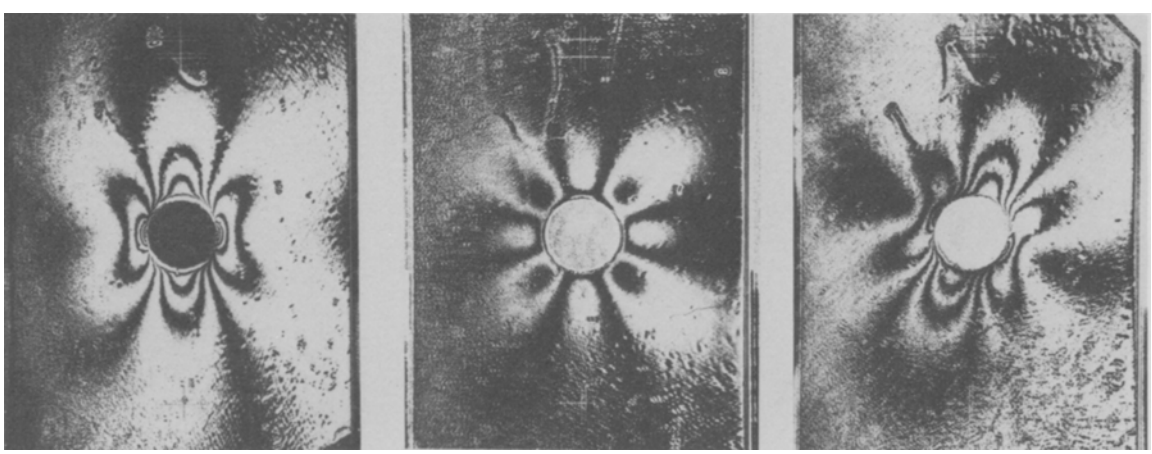

Fig. 7—Strain fringes N'_x, N'_y, N'_{45} (left to right) by mechanical shearing, with shear distance of 0.64 mm (0.025 in.)

$$\Delta U_x = (1/f_1)\Delta N_x \qquad (2a)$$

where f_1 is frequency of the (virtual) reference grating, and since

$$\epsilon_x = \partial U_x/\partial x \simeq \Delta U_x/\delta_x \qquad (3)$$

where ΔU_x is the local change of specimen displacement between two points that are δ_x apart,

$$\Delta U_x/\delta_x = (1/f_1)\Delta N_x/\delta_x = (1/f_1)N_x'/\delta_x$$

Thus,

$$\epsilon_x = \frac{N_x'}{f_1\delta_x}; \qquad \epsilon_y = \frac{N_y'}{f_1\delta_y}; \qquad \epsilon_{45} = \frac{N_{45}'}{f_2\delta_{45}} \qquad (4)$$

where N' represents fringe orders in the patterns of Fig. 7. They are approximations which approach the exact values as $\delta \to 0$. However, N' is proportional to δ with this method, so some choice of finite δ is required.

Shearing translation δ was 0.64 mm (0.025 in.) for the patterns of Fig. 7. The approximation is similar to that inherent in an electrical-resistance strain gage of 0.64-mm (0.025-in.) gage length.

Figure 8 shows the effect of increasing δ to 1 mm (0.040 in.) for the ϵ_y pattern. In cases where the strain gradient is small, it is often useful to increase the shearing distance and thus increase the number of fringes in the pattern.

The initial pattern of Fig. 4 generates an apparent initial strain field, too, which should be subtracted from the corresponding strain field of Fig. 7(a). The mechanical shearing technique was applied for this no-load condition to generate the pattern of Fig. 9. The apparent strain pattern is sparse, even though a much larger shearing distance of 3.2 mm (0.125 in.) was used. The small apparent strains of the no-load pattern caused the slight departures from symmetry seen in Fig. 7.

When interpreting these patterns, material points in the specimen should be assumed to lie midway between the corresponding points in the two superimposed images.

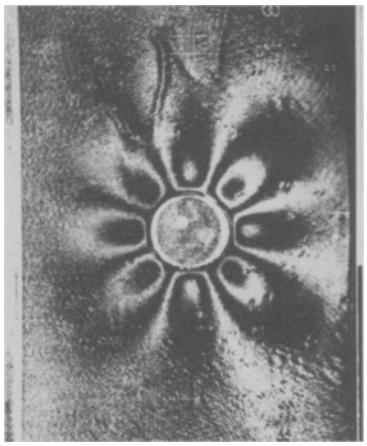

Fig. 8—Strain fringes N_y' with shearing distance of 1 mm (0.040 in.)

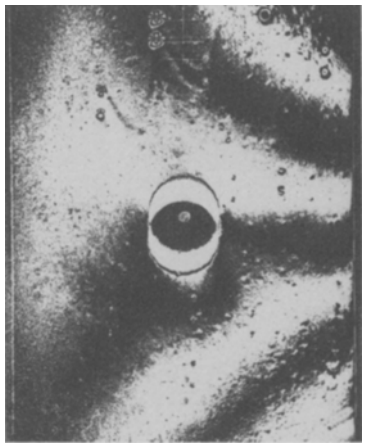

Fig. 9—Initial strain field with shearing distance of 3.2 mm (0.125 in.)

Discussion

U_{45} Is A Dependent Variable

Displacement components U_x and U_y fully define the in-plane displacement of a point. Component U_{45} is a dependent variable, viz.,

$$U_{45} = \frac{\sqrt{2}}{2}(U_x + U_y) \qquad (5)$$

Displacement field U_{45} is not investigated to determine displacements for their own sake, but as a vehicle for the rosette method to determine strains.

Alternate Means of Strain Analysis

Three strains determine the complete state of strain at a point, ϵ_x, ϵ_y, γ_{xy}. The shear strain can be evaluated by cross-derivatives of displacements as

$$\gamma_{xy} = \frac{\partial U_x}{\partial y} + \frac{\partial U_y}{\partial x} \qquad (6)$$

This is in contrast to the rosette equation, eq (1), which can be evaluated with direct derivatives exclusively.

Rotational Mismatch

Rotational mismatch is the angular misalignment between lines on the specimen and reference gratings. With moiré interferometry—just as in coarse moiré—it is often difficult to control the rotational mismatch. In the special case of a symmetrical displacement field, the gratings can be adjusted to produce a symmetrical moiré pattern. Even in this case, however, the no-load pattern resulting from imperfect gratings may be nonsymmetrical. In the general problem, the degree of rotational mismatch is unknown.

Still, mismatch is of no consequence when identical mismatch occurs for the no-load and load patterns if they are subtracted in the data-reduction process. Accidental rigid-body rotations that are likely to occur in the loading process, however, produce data with unknown rotational mismatch.

Post[7] has shown that eq (4) can be used even with unknown rotational mismatch if the mismatch is identical in the U_x and U_y patterns. This, too, is difficult to control in many instances.

Rotational mismatch introduces fringes that bisect the perpendiculars to the specimen and reference gratings.

Since the rotational mismatch fringes result from a very small rotation—even when a dense carrier pattern is formed—the angle between the fringes and the perpendicular to the reference grating lines is negligible.

Superiority of the Rosette Method

The derivatives $\partial U_x/\partial x$ and $\partial U_x/\partial y$ can be written in terms of fringe orders of the displacement patterns, viz., $(1/f)\partial N_x/\partial x$ and $(1/f)\partial N_x/\partial y$, respectively. With translation δ made parallel to the fringes of the carrier pattern, the direct derivatives, e.g., $\partial N_x/\partial x$, remain unaffected by the fringes of rotational mismatch while the cross-derivatives, e.g., $\partial N_x/\partial y$, are critically sensitive to them.

Consequently, the method that uses direct derivatives exclusively is superior for most cases, specifically the rosette method.

Differentiation

Three direct derivatives must be determined for the rosette method. Various methods of differentiation may be utilized, including graphical differentiation, where (a) displacement curves are plotted from fringe data, (b) tangents are estimated and (c) their slopes are measured. In the present work, differentiation was performed by the mechanical shearing method, where derivatives are approximated by ratios of finite increments [e.g., eq (3)].

Comparison of Figs. 6 and 7 emphasizes that differentiation is an inefficient process. The great abundance of displacement contours in Fig. 6 is reduced to the sparse pattern of derivative contours in Fig. 7. This is inherent in the differentiation of experimental data regardless of the method employed. In a nonhomogeneous strain field, the derivative of displacements may be determined to a given accuracy (e.g., 90 percent) if the displacements are known to a superior accuracy (e.g., 99 percent). Various computer-assisted data-reduction systems can be employed to fit and smooth the experimental data, thereby improving the accuracy of displacement information and, consequently, their derivatives.

A distinct feature of the mechanical shearing method of differentiation lies in its full-field nature, where the derivative is simultaneously determined at all points in the field of view.

Two-beam Interference

Figure 6 illustrates that fringe densities as high as 12 fringes/mm (300 fringes/in.) were clearly resolved. The displacement fringes used for mechanical shearing had a 24 fringes/mm (600 fringes/in.) carrier pattern added to this. These, too, could be seen in the camera-film plane (with the aid of magnification) and the fringes were well resolved and had high contrast. This must be so, since the double exposure of this pattern and its sheared (or translated) twin produced the clear moiré patterns from which Fig. 7 was derived.

The method of moiré interferometry utilized here is the two-beam interferometry and has all the valuable attributes of two-beam interferometry. When sufficient coherent light is used, fringe order is virtually unlimited; fringe densities exceeding 100 per mm (2500 per in.) can be realized; fringe contrast is virtually independent of fringe order; and the fringes can always be viewed on the surface of the workpiece.

The importance of these qualities is underscored by the work of Parks[8] on speckle interferometry. Speckle interferometry and moiré interferometry have the same governing equations and the same sensitivity in displacement per fringe. Parks shows, however, that the speckle method suffers limitations associated with speckle correlation, namely, serious limitations of range, contrast and fringe localization. It is clear from the figures exhibited here that moiré interferometry does not suffer these limitations.

Further Work

Two refinements would be attractive: (1) means for continuously variable shearing displacements combined with simultaneous viewing of the fringes of strain components, and (2) means to provide results as fringe patterns of the load-induced strain components, i.e., the load minus no-load strain components. This research is being contemplated.

Conclusions

This work demonstrates the following qualities:

(1) A crossed phase grating can be interrogated at 45 deg to generate the U_{45} displacement field.

(2) Sensitivity corresponding to gratings of 1700 ℓ/mm (43,000 ℓ/in.) can be obtained, i.e., sensitivity of 1/1700 mm per fringe.

(3) Well defined displacement fringes of very high fringe orders and very large fringe densities can be generated by moiré interferometry.

(4) Full-field patterns of strain components can be produced by mechanical shearing (or optical differentiation) of the displacement patterns.

(5) Shearing distances can be very small, comparable to the gage length of very short electrical-resistance strain gages.

(6) The rosette approach circumvents the experimental difficulties associated with rigid-body rotations and accidental misalignment of the reference grating.

Acknowledgments

This work was supported by the National Science Foundation under Grant ENG-7824609 with Clifford J. Astill as NSF program director. This support, and the assistance of the staff of the Engineering Science and Mechanics Department at VPI & SU, is greatly appreciated.

References

1. Dantu, P., "Extension of the Moiré Method to Thermal Problems," EXPERIMENTAL MECHANICS, **4** *(3), 64-69 (1964).*

2. Chiang, F.P., "Moiré Rosette Method for Strain Analysis," *J. Eng. Mech. Div., Proc. A.S.C.E., 96 (EMG), 2385-2389 (1970).*

3. Duncan, J.P. and Sabin, P.G., "An Experimental Method for Recording Curvature Contours in Flexed Elastic Plates," EXPERIMENTAL MECHANICS, **5** *(1), 22-28 (1965).*

4. Post, D. and MacLaughlin, T.F., "Strain Analysis by Moiré Fringe Multiplication," EXPERIMENTAL MECHANICS, **11** *(9), 408-413 (Sept. 1971).*

5. Post, D., "Optical Interference for Deformation Measurements—Classical, Holographic and Moiré Interferometry," *Mechanics of Nondestructive Testing, Proc. edited by W.W. Stinchcomb, Plenum Publishing Corp., New York (1980).*

6. Post, D. and Baracat, W.A., "High-sensitivity Moiré Interferometry—A Simplified Approach," EXPERIMENTAL MECHANICS, **21** *(3), 100-104 (March 1981).*

7. Post, D., "The Moiré Grid Analyzer Method for Strain Analysis," EXPERIMENTAL MECHANICS, **5** *(11), 368-377 (1965).*

8. Parks, V.J., "The Range of Speckle Metrology," EXPERIMENTAL MECHANICS, **20** *(6), 181-191 (June 1980).*